

A Family of Integral Methods for Predicting Turbulent Boundary Layers

A. K. LEWKOWICZ*

Liverpool University, England

AND

D. HOADLEY,† J. H. HORLOCK,‡ AND H. J. PERKINS†

Cambridge University, England

A family of integral methods for predicting the development of two-dimensional incompressible turbulent boundary layers in arbitrary pressure gradients is described. The momentum integral equation and a wall friction relation are used in each method. A third equation must be selected from A) the energy integral equation, B) the entrainment equation, or C) the moment of momentum integral equation. It is shown that an over-all comparison of all three methods with a wide range of experimental results is generally satisfactory. The use of B gives the best agreement for adverse pressure gradient cases whereas the use of A and C predicts equilibrium and relaxing flows better.

Nomenclature

B	= law of the wall constant
$C(=K\theta)$	= three-dimensionality correction
c_f	= wall friction coefficient
D	= dissipation integral
E	= entrainment function
G_1, G_2, \dots, G_9	= polynomial functions of Π
$H(=\delta^*/\theta)$	= mean velocity shape factor
$H_{\delta-\delta^*}$	
$[(\delta - \delta^*)/\theta]$	= mean velocity shape factor
K	= curvature of normals to external streamlines
k	= von Kármán constant
$R\theta(=U_\infty\theta/\nu)$	= Reynolds number based on momentum thickness
S	= shear stress integral
U	= boundary-layer mean velocity in x direction
U_∞	= freestream velocity
$\rho u v$	= turbulent shear stress
W	= Coles' universal wake function
x	= longitudinal coordinate
y	= transverse coordinate (across boundary layer)
α	= eddy viscosity proportionality constant (in outer region)
δ	= absolute thickness of boundary layer
δ^*, δ^{**}	= displacement and energy thicknesses, respectively
ϵ	= eddy viscosity coefficient
ϵ_i	= eddy viscosity coefficient in inner region
ϵ_o	= eddy viscosity coefficient in outer region
η	= nondimensional transverse coordinate
η_o	= value of η at the boundary between inner and outer regions
θ	= momentum thickness
μ	= dynamic viscosity
ν	= kinematic viscosity
Π	= Coles' parameter
ρ	= density
τ	= total shear stress
τ_w	= wall shear stress
$\omega[(c_f/2)^{1/2}]$	= wall friction coefficient

1. Introduction

BOUNDARY-layer problems may be solved by direct integration of the equations of motion. Except for the simplest cases analytical solutions cannot be obtained. In laminar boundary layers the problem is well defined but for turbulent boundary layers the unknowns exceed in number the governing equations and some degree of empiricism must be introduced. This empirical information usually relates turbulent quantities to the mean flow. Relatively crude models for the wall turbulence have been suggested, such as the eddy viscosity concept or the mixing length hypothesis. Such models have been used in the direct integration methods of Mellor,¹ Smith and Cebeci,² and Patankar and Spalding.³ Bradshaw et al.⁴ have employed the turbulent kinetic energy equation, thereby taking into account the effects of the turbulence structure. These methods have to a certain extent overshadowed recent developments in integral methods. The latter are based on more empirical assumptions but are easier to use. A demand still exists for a fast, simple method of calculating boundary layers which may be included as a subroutine to an inviscid flow computer program.

A particular family of integral methods is described below and the results of computed examples are presented. Three variants of the basic procedure are described, each using the momentum integral and a wall friction relation, but each using a different third equation, which in the present case is selected from the following: the energy integral equation, the entrainment equation, and the moment of momentum integral equation. Each set of three equations is solved simultaneously for three boundary-layer parameters, following the method developed by Lewkowicz and Horlock⁵ and also used by Hirst and Reynolds.⁶ It has been found that the selection of the third equation and the consistency of the starting values are important for numerical stability and convergence. An extension of the method for calculating three-dimensional flows is outlined in Appendix C.

An earlier, less versatile, version of the family of integral methods was presented at the recent 1968 AFSOR-IFP Stanford Conference on Computation of Turbulent Boundary Layers and has been published in the Conference Proceedings (Vol. 1). The present paper deals with a more general approach and utilizes more stringent convergence criteria which result in a markedly improved accuracy. The Stanford version did not include the moment of momentum alternative.

Received December 6, 1968; revision received May 26, 1968.

* Lecturer, Mechanical Engineering Department. Member

AIAA.

† Research Student, Engineering Department.

‡ Professor of Engineering, Engineering Department.

2. General Theory

The following boundary-layer equations are well established (for further details see, e.g., Rotta⁷ and Head⁸).

2.1 Integral Equations

The momentum integral equation:

$$\frac{d\theta}{dx} + \frac{1}{U_\infty} \frac{dU_\infty}{dx} (2\theta + \delta^*) = \omega^2 \quad (1)$$

The energy integral equation:

$$\frac{1}{2U_\infty^3} \frac{d}{dx} (U_\infty^3 \delta^{**}) = \frac{1}{\rho U_\infty^3} \int_0^\infty \tau \frac{\partial U}{\partial y} dy (=D) \quad (2)$$

The moment of momentum integral equation:

$$\frac{1}{U_\infty^2} \frac{d}{dx} \left[U_\infty^2 \int_0^\infty y \left(1 - \frac{U}{U_\infty} \right) \frac{U}{U_\infty} dy \right] + \frac{1}{U_\infty} \int_0^\infty \left(1 - \frac{U}{U_\infty} \right) \frac{d}{dx} \left[U_\infty \left(y + \int_0^y \frac{U}{U_\infty} dy \right) \right] dy = \frac{1}{\rho U_\infty^2} \int_0^\infty \tau dy (=S) \quad (3)$$

The entrainment equation:

$$\frac{1}{U_\infty} \frac{d}{dx} [U_\infty (\delta - \delta^*)] = E \quad (4)$$

The turbulent normal stress terms have not been included in the first three equations, although it is appreciated that they may be significant near separation. The conventional boundary-layer thicknesses are defined by

$$\delta^* = \int_0^\infty \left(1 - \frac{U}{U_\infty} \right) dy \quad \text{displacement thickness} \quad (5a)$$

$$\theta = \int_0^\infty \frac{U}{U_\infty} \left(1 - \frac{U}{U_\infty} \right) dy \quad \text{momentum thickness} \quad (5b)$$

$$\delta^{**} = \int_0^\infty \frac{U}{U_\infty} \left[1 - \left(\frac{U}{U_\infty} \right)^2 \right] dy \quad \text{energy thickness} \quad (5c)$$

The wall friction coefficient is given by

$$c_f = \frac{\tau_w}{\frac{1}{2} \rho U_\infty^2} = 2\omega^2$$

2.2 Velocity Profile

If the sublayer is excluded, a turbulent boundary-layer velocity profile is well represented by the law of the wall and the law of the wake (c.f. Coles⁹);

$$\frac{U}{\omega U_\infty} = \frac{1}{k} \log_e \frac{y \omega U_\infty}{\nu} + \frac{\Pi}{k} W \left(\frac{y}{\delta} \right) + B \quad (6)$$

Here the quantities δ , Π , and ω referred to hereafter as the dependent variables, may change with the streamwise coordinate x , and $W(y/\delta)$ is a universal wake function tabulated by Coles. An analytical expression for the wake function was suggested by Hinze,¹⁰

$$W(y/\delta) = 1 - \cos(\pi y/\delta) \quad (7)$$

The Coles profile may also be written in its velocity defect form for evaluating the boundary-layer thicknesses and the form parameters listed in Appendix A,

$$\frac{U_\infty - U}{U_\infty} = \frac{\omega}{k} \left\{ \Pi \left[2 - W \left(\frac{y}{\delta} \right) \right] - \log_e \frac{y}{\delta} \right\} \quad (8)$$

2.3 Wall Friction Equation

A well-established empirical expression for the wall friction is the Ludwig and Tillmann equation,

$$\omega^2 = 0.123 \times 10^{-0.678H} (\theta U_\infty / \nu)^{-0.268} \quad (9)$$

where the conventional form parameter $H = \delta^*/\theta$. This was used in preliminary calculations. It is more consistent to use a friction law derived from the Coles profile. By putting $y = \delta$ at $U = U_\infty$ in Eq. (6), an implicit equation for ω is obtained,

$$\frac{1}{\omega} - \frac{1}{k} \log_e \omega = \frac{1}{k} \log_e \left(\frac{\delta U_\infty}{\nu} \right) + \frac{2\Pi}{k} + B \quad (10)$$

which was shown by Kawasaki¹¹ to be almost identical with the Ludwig and Tillmann relation. The wall friction law, Eq. (10), was used in the calculations described here.

2.4 Expressions for the Dissipation Integral, Shear Stress Integral, and Entrainment

Empirical information is required in determining the dissipation integral D and the shear stress integral S appearing in Eqs. (2) and (3), respectively. The most advanced way of dealing with D and S is by using empirical and theoretical knowledge of the structure of wall turbulence. In consequence, one could utilize the correlation equations for the turbulent stresses (or for the turbulent kinetic energy). However, for simplicity, the integrals D and S in the present work were related to the dependent variables δ , Π , and ω through the turbulent shear stress distribution evolving from the well-known two-layer eddy viscosity concept of Clauser.¹² It is assumed that this model, derived originally for equilibrium boundary layers, may be used for more general cases. The authors are aware of its limitations.

Details of the derivation of D and S are given in Appendix B, the final expressions being

$$D = \omega^2 + \frac{\omega^3}{k} \left\{ 1 + \log_e \eta_o - \eta_o + 2\Pi \times \left(1 - \cos(\pi \eta_o) + \pi \eta_o \sum_{n=1}^{\infty} \frac{(-1)^{n-1} \pi^{2n-1} (1 - \eta_o^{2n-1})}{(2n-1)(2n-1)!} \right) + \frac{\Pi^2}{2} \left[\pi^2 \eta_o \left(1 - \frac{\eta_o}{2} \right) + \frac{\sin^2(\pi \eta_o)}{4} \right] \right\} \quad (11)$$

$$S = \delta \omega^2 \left[\eta_o (1 + \Pi - \log_e \eta_o) + \frac{\Pi}{\pi} \sin(\pi \eta_o) \right] \quad (12)$$

where $\eta_o = \alpha(1 + \Pi)/k^2$ and α is a constant determining the magnitude of the eddy viscosity in the outer region. The value η_o defines the point within the boundary layer where the inner and outer regions join together.

The nondimensional entrainment E in Eq. (4) is assumed to depend only upon a form parameter $H_{\delta-\delta^*} = (\delta - \delta^*)/\theta$ as suggested by Head.⁸ An analytical approximation to Head's original curve is

$$E = 0.0306(H_{\delta-\delta^*} - 3)^{-0.653} \quad (13)$$

The rate of entrainment depends primarily on the turbulent structure of the flow. Head relates the entrainment to mean flow quantities through an empirical expression which implicitly accounts for at least some of the effects of turbulence. The turbulence was explicitly taken into account in a more fundamental way by Hirst and Reynolds,⁶ who used the turbulent kinetic energy equation, in its integral form, to relate the entrainment to a characteristic turbulent velocity scale.

All the foregoing quantities, D , S , and E , could be biased more towards the past history of the boundary-layer development by forming a crude rate of development relation,

$$\frac{dX}{dx} = \frac{\text{const}}{\delta} (X_{eq} - X)$$

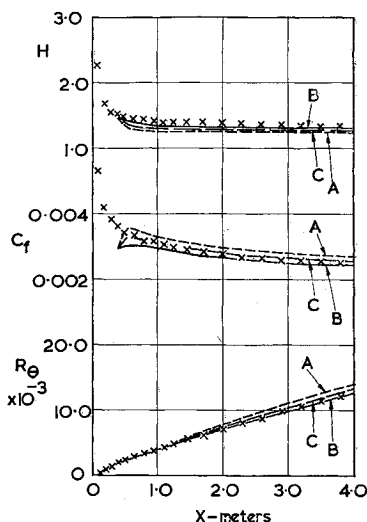


Fig. 1 Constant pressure flow (Wiegardt 1400); A—energy, B—entrainment, C—moment.

where $X \equiv D$, $X \equiv S$, $X \equiv E$ for the energy equation, the moment of momentum equation, and the entrainment equation, respectively; the quantity X_{eq} corresponds to the value of X inherent in equilibrium boundary layers and as such is likely to depend on Π only.

Some authors have used this relation (for example Goldberg,¹³ McDonald,¹⁴ and Nash¹⁵) but almost invariably this procedure, and that of Hirst and Reynolds,⁶ lead to difficulties in choosing the initial values for those boundary layers where the initial stage is not an equilibrium flow.

2.5 Expressions for the Boundary-Layer Thickness and the Coles Wake Parameter

The usual definition of the absolute boundary-layer thickness is $\delta = y$ at $U = 0.995U_\infty$. This is not very satisfactory for the present type of analysis. An exact analytical expression for the absolute thickness can be obtained by substituting Eq. (8) with Eq. (7) in Eq. (5a), giving

$$\delta = \frac{k\delta^*}{\omega(1 + \Pi)} \quad (14)$$

By using Eqs. (7, 8, 5a, and 5b), the Coles wake parameter Π may be related to the measurable form parameter H and the wall friction parameter ω by

$$1.5\Pi^2 + \left(3.179 - \frac{k}{\omega} \frac{H-1}{H}\right)\Pi + \left(2 - \frac{k}{\omega} \frac{H-1}{H}\right) = 0 \quad (15)$$

Equation (15) is used for evaluating the initial value of Π .

2.6 Equation in Terms of the Coles Parameters

The integral equations [(1), (2), (3), and (4)] may be transformed into four ordinary differential equations for δ , Π , and ω . This is done by evaluating δ^* , θ , and δ^{**} in the integral equation in terms of δ , Π , and ω by introducing Eq. (8) into Eqs. (5).

Momentum integral equation:

$$(G_1 - \omega G_2)\omega \frac{d\delta}{dx} + \left(\frac{1}{k} - \omega G_3\right)\omega \delta \frac{d\Pi}{dx} + (G_1 - 2\omega G_2)\delta \frac{d\omega}{dx} = \omega^2 - \frac{1}{U_\infty} \frac{dU_\infty}{dx} (3G_1 - 2\omega G_2)\omega \delta \quad (16)$$

§ Equation (14) has not been corrected for the inconsistencies reported by Bull²⁴ which are associated with the freestream boundary conditions for the Coles velocity profile in its defect form. Bull's paper was published after the present article had been submitted for publication.

Energy integral equation:

$$(G_1 - 1.5\omega G_2 + \omega^2 G_4)\omega \frac{d\delta}{dx} + \left(\frac{1}{k} - 1.5\omega G_3 + \omega^2 G_5\right)\omega \delta \frac{d\Pi}{dx} + (G_1 - 3\omega G_2 + 3\omega^2 G_4)\delta \frac{d\omega}{dx} = \omega^2 - \frac{1}{U_\infty} \frac{dU_\infty}{dx} \times (3G_1 - 4.5\omega G_2 + 3\omega^2 G_4)\omega \delta + \frac{\omega^3}{k} \left(1 + \log_e \left(\frac{\alpha}{k} G_1\right) - \frac{\alpha}{k} G_1 + 2\Pi \left[1 - \cos\left(\pi \frac{\alpha}{k} G_1\right) + \pi \frac{\alpha}{k} G_1 \sum_{n=1}^{\infty} \frac{(-1)^{2n-1} \{1 - [(\alpha/k)G_1]^{2n-1}\}}{(2n-1)(2n-1)!}\right] + \frac{\Pi^2}{2} \left\{\pi^2 \frac{\alpha}{k} G_1 \times \left(1 - \frac{\alpha G_1}{2k}\right) + \frac{\sin^2[\pi(\alpha/k)G_1]}{4}\right\}\right) \quad (17)$$

Moment of momentum integral equation:

$$(2G_6 - \omega G_7)\omega \frac{d\delta}{dx} + \left(\frac{0.294}{k} - \omega G_8\right)\omega \delta \frac{d\Pi}{dx} + (G_6 - \omega G_9)\delta \frac{d\omega}{dx} = -\frac{1}{U_\infty} \frac{dU_\infty}{dx} (4G_6 - \omega G_9)\omega \delta + \omega^2 \left\{\frac{\alpha}{k} G_1 \left[1 + \Pi - \log_e \left(\frac{\alpha}{k} G_1\right)\right] + \frac{\Pi}{\pi} \sin\left(\pi \frac{\alpha}{k} G_1\right)\right\} \quad (18)$$

Entrainment equation:

$$(1 - \omega G_1) \frac{d\delta}{dx} - \frac{\omega \delta}{k} \frac{d\Pi}{dx} - G_1 \delta \frac{d\omega}{dx} = -\frac{1}{U_\infty} \frac{dU_\infty}{dx} \times (\delta - \omega \delta G_1) + 0.0306 \left(\frac{1 - \omega G_1}{\omega G_1 - \omega^2 G_2} - 3\right)^{-0.653} \quad (19)$$

In these equations the G functions are functions of Π and the von Kármán constant k and are listed in Appendix A.

For numerical convenience, the wall friction relation, Eq. (10), should be differentiated with respect to x , giving

$$\frac{1}{\delta} \frac{d\delta}{dx} + 2 \frac{d\Pi}{dx} + \left(\frac{1}{\omega} + \frac{k}{\omega^2}\right) \frac{d\omega}{dx} = -\frac{1}{U_\infty} \frac{dU_\infty}{dx} \quad (20)$$

A similar equation may also be obtained from the Ludwig and Tillmann wall friction law, Eq. (9), as shown by Lewkowicz and Horlock.⁵

2.7 Choice of the Three Differential Equations

The state of a boundary layer at any streamwise station x is adequately described by the dependent variables δ , Π , and ω . Three differential equations are required if a solution in terms of these parameters is to be obtained. The equations available are: the momentum equation, Eq. (16); the energy equation, Eq. (17); the moment of momentum equation, Eq. (18); the entrainment equation, Eq. (19); and the wall friction equation, Eq. (20).

Initially a solution was attempted in which Eqs. (16, 17, and 18) were used but it was found that stable solutions could not be obtained. It was therefore decided to introduce a wall friction relation instead of the moment of momentum equation. Equations (16, 17, and 20) thus form the basis of method A, denoted the energy method.

It was found subsequently that method A was sensitive to the initial conditions and the selection of the constant α for the eddy viscosity in the outer part of the boundary layer (for further discussion see Appendix B). It was therefore decided to introduce the entrainment equation (19) instead of the energy equation. Thus the basis of method B—the entrainment method—is the simultaneous solutions of the momentum equation (16), the entrainment equation (19), and the Coles wall friction relation, Eq. (20).

It is shown in the next section that predictions of method B are for some cases closer to the experimental data than those

of method A. It was realized subsequently that the shortcoming of method A may be due to a numerical difficulty in solving the differential equations. The energy equation is obtained by multiplying the basic momentum equation by the local velocity U . However, as noted by Hirst and Reynolds,⁶ U approaches the freestream velocity U_∞ asymptotically over a substantial part of the boundary layer, so that the coefficients of $d\delta/dx$, $d\Pi/dx$, and $d\omega/dx$ in the energy equation are little different from those in the momentum equation [compare Eq. (16) with Eq. (17) remembering that ω is small]. On the other hand, the coefficients in the moment of momentum equation (18) are different from those in Eq. (17), since this equation is derived by integrating the product of the basic momentum equation with y and not U . A more stable solution should therefore be achieved by combining the momentum equation (16), moment of momentum equation (18), and the Coles wall friction equation (20), and this is the basis of method C—the moment method.

3. Calculation of Examples

A very comprehensive set of data from boundary-layer experiments has been compiled by Coles and Hirst¹⁶ and formed the basis for comparison with the calculations submitted by many workers at the 1968 AFOSR-IFP Stanford Conference. The integral quantities and wall friction at each longitudinal station are presented together with the streamwise distribution of velocity and velocity gradient. Eight of these flows have been calculated by each of the three methods and H , c_f , and R_θ predicted. It is considered that these eight examples constitute a reasonable test of a boundary-layer prediction method. The notation is that of Coles and Hirst¹⁶ and details of the experiments will be found in their review.

3.1 Method of Solution

FORTRAN IV was used to program all three methods for the IBM 1130 machine at the Cambridge University Engineering Department. Standard subroutines were used to solve simultaneously step by step each set of three equations for δ , Π , and ω by a Runge-Kutta technique. For each flow calculation the initial values of δ , Π , and ω at the starting station must be fed in as data, together with the velocity and velocity gradient at each computation step. A subroutine was written for parabolic interpolation between data values of U_∞ and dU_∞/dx . Typical run times on the 1130 machine were 1.5 min per flow including the printout (without a line printer).

3.2 Initial Conditions and Convergence of Solution

To start a calculation the initial values of δ , Π , and ω are required. These parameters are not, however, independent and one may always be expressed in terms of the other two by Eq. (10). Although the wall constant B in the Coles relation, Eq. (10), disappears under differentiation to give Eq. (20) a value must be chosen at the starting point which should remain constant during the calculation. For the Stanford Conference, starting values of H , c_f , and R_θ were given. There are then two possible ways of beginning a calculation. The three starting values may be converted into δ , Π , and ω and a corresponding value of B determined for that calculation, which in the case of mismatched initial conditions may lead to an unrealistic value of B . Alternatively, a "universal" value of B may be assumed, together with two of the given starting values and an alternative starting value of the remaining variable determined. For the calculations described below the second approach was followed, using a value of $B = 4.9$ and the associated von Kármán constant $k = 0.41$. The given values of H and R_θ were then used to calculate the initial value of c_f . An iterative

procedure was used to find the initial values of the dependent variables from Eq. (10) and the expressions for H and θ given in Appendix A.

The value of B should not change at each step in the calculation. A ready means of ensuring that the solution is converging is therefore to calculate B after each step from the local values of the dependent variables and to halve the step until B attains its given value within a specified tolerance. Except for two flows the tolerance on B for the calculations described here was ± 0.05 . For the Schubauer and Klebanoff flow 2100 and the Moses 5 flow 4000 this tolerance had to be relaxed to ± 0.1 to achieve a reasonable minimum number of iterations over the whole calculation.

By appropriate choice of B , the surface roughness can be accounted for and if such a roughness varies longitudinally then its variation must be prescribed within the input as $B(x)$.

The predictions of method B, and of method A using the Ludwig and Tillmann relation, Eq. (9), instead of Eq. (10), were submitted to the 1968 AFOSR-IFP Stanford Conference. For those calculations the three initial values recommended by Coles and Hirst were used, but without a check on B . With these values the inconsistency of one of the governing equations, in this case the wall friction relation, is thought to be the cause of poor predictions in some cases of both these two methods (and calculations by other methods submitted to the Conference).

3.3 Empirical Constants

A number of empirical constants and functions appear in each of the three methods. The constants in the law of the wall in Eq. (10) have been commented upon in the preceding section. In methods A and C a value for α appearing in the Clauser eddy viscosity model, described in Appendix B, has to be chosen. Although it is likely that α will vary with the pressure gradient and past history of the flow, the same value of $\alpha = 0.018$ was used in all the calculations. In method B the entrainment function E was assumed to follow the curve given by Head⁸ and was used for all the calculations described here.

3.4 Three-Dimensional Corrections

In some of the experimental flows used here there is a possibility of divergent, or convergent, streamlines in the freestream. The two-dimensional predictions of R_θ given by the three methods then disagree with the experimental points. In flows with adverse pressure gradients, some of the momentum transfer is due to the normal turbulent stresses, which are neglected in Eqs. (1, 2, and 3). Some account of them can be made in an empirical way as shown by Lewkowicz and Horlock⁵ and Goldberg.¹³ However, early calculations using method A showed that the normal stress term had little effect except near separation. A correction for three dimensionality was made to the momentum equation (1) and entrainment equation (4) in method B, assuming that the normal stresses were negligible. The momentum imbalance data of Coles and Hirst¹⁶ were used (although these data were somewhat erratic), and the technique is described in Appendix C.

3.5 Comments on the Predictions

Predictions of H , c_f , and R_θ by each of the methods for the eight experimental flows are displayed in Figs. 1–8. The experiments chosen here are not necessarily those that offer the best agreement with the present theory. It is considered that they cover a reasonably wide range of possible turbulent boundary-layer flows. The effect of the three-dimensional correction in method B on three of the flows is shown in Figs. 9–11 as curves D.

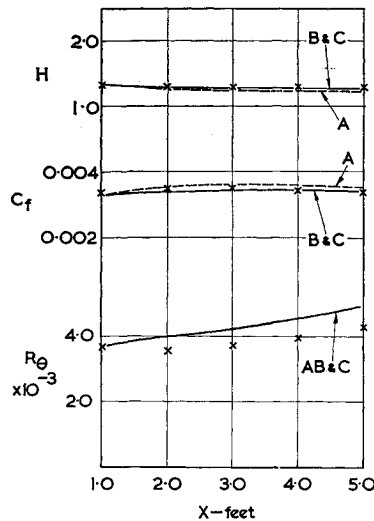


Fig. 2 Equilibrium flow in a negative pressure gradient (Herring and Norbury 2700); A—energy, B—entrainment, C—moment.

Method A is quite good for equilibrium flows and fair for adverse pressure gradient flows and relaxing flows. In calculations not shown here values of α other than 0.018 gave better agreement with some of the experimental results. Because of the similarity of coefficients in the momentum and energy equations (16) and (17), the selection of α and the initial values of the dependent variables are somewhat critical for insuring numerical stability and consistency. The complicated expression for the dissipation integral, Eq. (11), caused method A to require the longest computation time. Method B gives better predictions of flows with severe adverse pressure gradients but could not predict the Moses relaxing flow. Method C is also quite good for equilibrium flows and is less sensitive to choice of α than method A.

It is not surprising that methods A and C agree with equilibrium flows well, since their inherent dissipation and shear stress integrals, respectively, are based on the Clauser eddy viscosity concept which itself originates from equilibrium turbulent boundary layers. The same argument applies to method B whose entrainment function was derived from flows with severe pressure gradients.

None of the methods could predict the Moses relaxing flow exactly. This deficiency of all the methods is probably due to inadequate representation of the past history element (see Sec. 2.4).

The inclusion of three-dimensional correction terms in method B shows the importance of taking into account the convergence or divergence of the external flow. As pointed out by Bradshaw and Ferriss,¹⁷ the H development is not affected unless the correction is substantial.

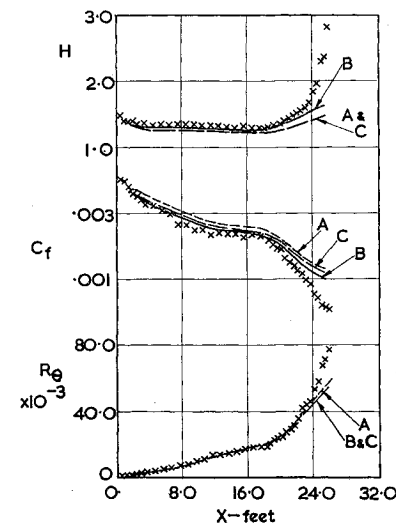


Fig. 3 Aerofoil flow with severe positive pressure gradient (Schubauer and Klebanoff 2100); A—energy, B—entrainment, C—moment.

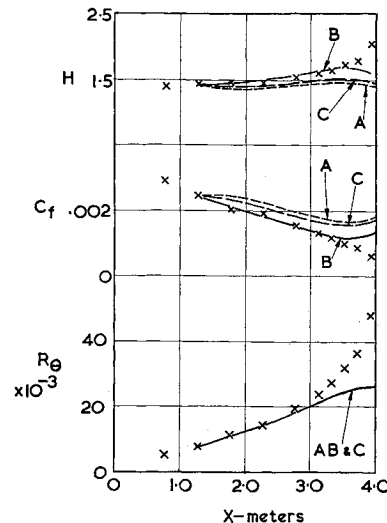


Fig. 4 Flow in a severe positive pressure gradient (Ludwig and Tillmann 1200); A—energy, B—entrainment, C—moment.

4. Conclusions

A family of integral methods for calculating two-dimensional turbulent boundary layers has been developed and three variants compared. It is concluded that integral methods which solve for the parameters δ , Π , and ω , as described here, are adequate for most engineering purposes, but only if the governing differential equations do not have similar coefficients. The initial values of the parameters required to start a calculation must be consistent with the integrated form of the equations.

The authors consider that all three methods could be improved further by consistent inclusion of the three-dimensional effects and by accounting for the normal turbulent stresses.

Appendix A: Functions of the Dependent Variables

$$\delta^* = \omega \delta G_1$$

$$\theta = \omega \delta G_1 - \omega^2 \delta G_2$$

$$\delta^{**} = 2\omega \delta G_1 - 3\omega^2 \delta G_2 + 2\omega^3 \delta G_4$$

$$H = G_1 / (G_1 - \omega G_2)$$

$$H_{\delta-\delta^*} = (1 - \omega G_1) / (\omega G_1 - \omega^2 G_2)$$

Using the Hinze approximation to the wake function, Eq. (7), in the Coles velocity defect law Eq. (8), the preceding G

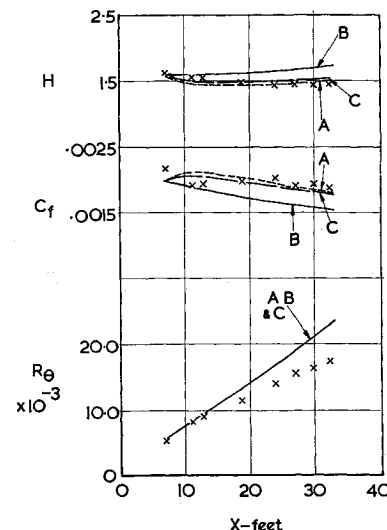
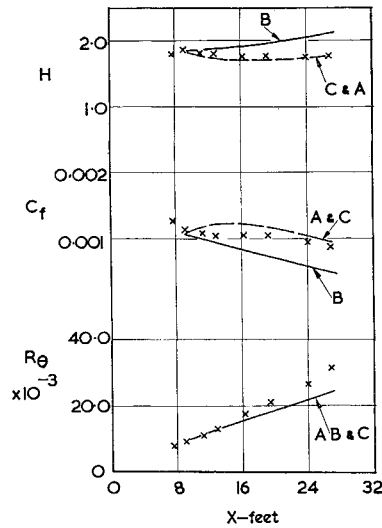


Fig. 5 Equilibrium flow in a positive pressure gradient (Clauser I 2200); A—energy, B—entrainment, C—moment.

Fig. 6 Equilibrium flow in a positive pressure gradient (Clauser II 2300); A—energy, B—entrainment, C—moment.



functions become

$$G_1 = \frac{1}{k} (1.0 + \Pi)$$

$$G_2 = \frac{1}{k^2} (2.0 + 3.179\Pi + 1.5\Pi^2)$$

$$G_3 = \frac{1}{k^2} (3.179 + 3.0\Pi)$$

$$G_4 = \frac{1}{k^3} (3.0 + 5.575\Pi + 4.25\Pi^2 + 1.281\Pi^3)$$

$$G_5 = \frac{1}{k^3} (5.575 + 8.5\Pi + 3.843\Pi^2)$$

Additional G functions appearing in the moment of momentum integral equation are

$$G_6 = \frac{1}{k} (0.25 + 0.2974\Pi)$$

$$G_7 = \frac{1}{k^2} (0.75 + 1.5713\Pi + 0.8447\Pi^2)$$

$$G_8 = \frac{1}{k^2} (0.9883 + 1.1894\Pi)$$

$$G_9 = \frac{1}{k^2} (1.0 + 2.1426\Pi + 1.1894\Pi^2)$$

Fig. 7 Relaxing flow (Bradshaw 2400); A—energy, B—entrainment, C—moment.

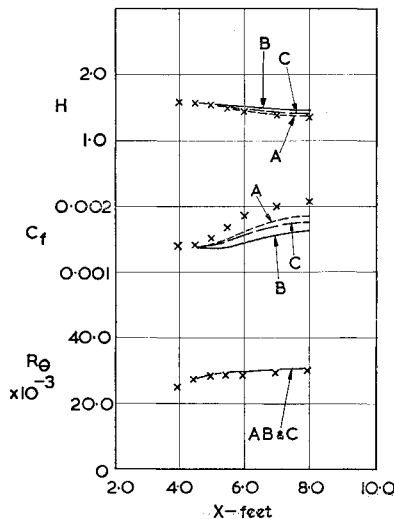
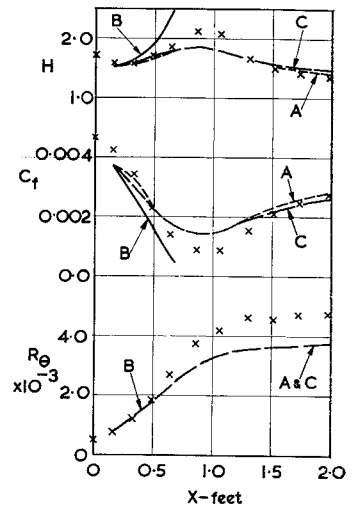


Fig. 8 Relaxing flow (Moses 5 4000); A—energy, B—entrainment, C—moment.



Appendix B: Dissipation and Shear Integrals

The dissipation integral D in Eq. (2) and the shear stress integral S in Eq. (3) are evaluated in terms of the dependent variables using Clauser's¹² two-layer eddy viscosity model. This model was originally suggested for equilibrium flows and relates the turbulent shear stress to the mean flow.

The total shear stress τ is the sum of its viscous and turbulent components,

$$\tau = \mu(\partial U/\partial y) + \rho(-\overline{uv})$$

the former usually being ignored. The eddy viscosity concept assumes that

$$-\overline{uv} = \epsilon(\partial U/\partial y)$$

In the Clauser model the eddy viscosity in the outer region of the boundary layer is constant and can be specified by

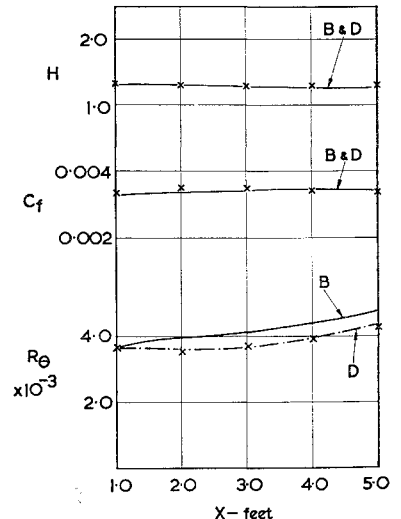
$$\epsilon_o = \alpha U_\infty \delta^*$$

where α is a constant. In the inner region the eddy viscosity varies linearly with y and is given by

$$\epsilon_i = k\delta U_\infty \omega \eta$$

where k is the von Kármán constant and $\eta = y/\delta$. Equating ϵ_o to ϵ_i gives η_o , the value of η at the boundary between the inner and outer regions. The integration for D and S may now be carried out using Cole's profile, Eq. (8), with Hinze's wake function, Eq. (7). There are basically two regions of integration: the region $\eta_o < \eta < 1$ using ϵ_o and the region $0 < \eta < \eta_o$ where ϵ_i is appropriate. However,

Fig. 9 Three-dimensional correction to method B (Herring and Norbury 2700); B—uncorrected, D—corrected.



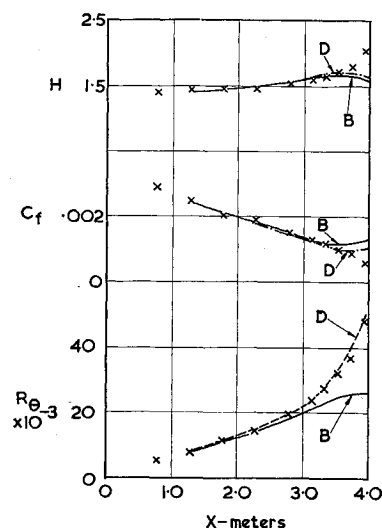


Fig. 10 Three-dimensional correction to method B (Ludwig and Tillman 1200); B—uncorrected, D—corrected.

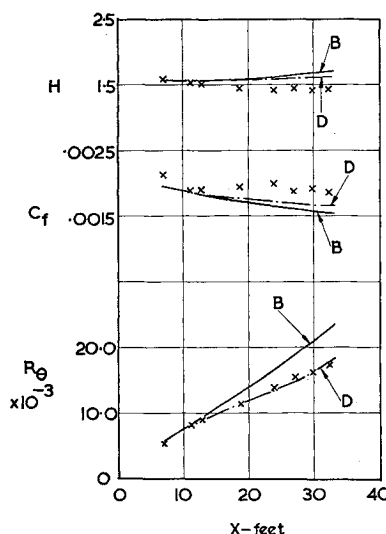


Fig. 11 Three-dimensional correction to method B (Clauser I 2200); B—uncorrected, D—corrected.

for the integral D a special subrange $0 < \eta < \eta'$ (where the shear stress is assumed constant and equal to τ_w , its value at the wall) must be chosen in order to avoid the logarithm of zero in the result. The subrange covers the entire viscous sublayer and the terms containing η' cancel. The final expressions for D and S are given by Eqs. (11) and (12).

The value of α is in fact likely to vary with the development of a particular flow. Townsend¹⁸ showed that for equilibrium flows there is a weak dependence of α on the pressure gradient parameter. The values of α at the first few stations of the flows calculated here were found directly from the predictions of shear stress by method B using the momentum equation integrated to any ordinate y . These values ranged from 0.012 to 0.022 with a definite concentration in the interval 0.015–0.020. A recommended value of α is therefore 0.018 and this was used in all the calculations of methods A and C.

Appendix C: Three-Dimensional Boundary Layers

The three-dimensional boundary-layer equations may be written in a streamline coordinate system on a surface of small curvature as shown by Cooke and Hall.¹⁹ If the crossflow is small, the crosswise derivatives may be neglected and the resulting system of four ordinary differential equations solved for the dependent variables and β , the limiting streamline angle at the wall, provided a family of crossflow velocity profiles is assumed. Using this procedure, Lewkowicz²⁰ calculated the boundary on a flat plate in a curved duct, and Wakhaloo²¹ predicted the end wall boundary layer in a compressor cascade passage, the three-dimensional energy integral equation being used in both cases. In axisymmetric flows the crosswise derivatives may be related to the streamwise derivatives and restriction to small crossflows is not necessary. Under these conditions Hoadley²² has calculated the boundary layers in an annular diffuser containing a swirling flow, using the three-dimensional entrainment equation derived by Cumpsty and Head.²³ In all cases the Prandtl-Mager quadratic law has been assumed for the crossflow profiles.

For the two-dimensional flows calculated here any experimental three dimensionality generally manifests itself in a convergence or divergence of the external streamlines, which have very small curvature. The crossflow terms in the three-dimensional equations may then be dropped and the momentum integral and entrainment equations (1) and (4) become

$$\frac{d\theta}{dx} + \frac{1}{U_\infty} \frac{dU_\infty}{dx} (2\theta + \delta^*) - K\theta = \omega^2$$

$$\frac{1}{U_\infty} \frac{d}{dx} [U_\infty (\delta - \delta^*)] - K(\delta - \delta^*) = E$$

Here K is the convergence and may be thought of as the reciprocal of the radius of curvature of the normals, or potential lines, to the streamlines.

By normalizing and integrating the two dimensional momentum integral equation (1), Coles and Hirst¹⁶ evaluated the momentum imbalance (PL-PR) from the experimental data for each run. If it is assumed that the momentum imbalance is due only to convergence and not to the turbulent normal stresses and/or streamwise curvature normal to the wall, then the required correction is given by

$$C = K\theta = \frac{(U_\infty^2 \theta)_0}{U_\infty^2} \frac{d}{dx} (PL - PR)$$

where the subscript 0 refers to the initial conditions. The correction term in the entrainment equation is now $CH_{\delta-\delta^*}$ and can be expressed in terms of δ , Π , and ω . A quartic in x was fitted by the method of least squares to the (PL-PR) points for each run and the slope evaluated to give C at each step in the computation procedure.

It should be noted that the convergence correction to the momentum integral equation as evaluated here takes into account all effects causing a momentum imbalance. The predictions of R_θ are forced to be correct. However, the correction to the entrainment equation is made under the assumption that only three-dimensional effects are present. Corrections to the energy integral equation and the moment of momentum equation may be carried out in a similar manner.

References

- ¹ Mellor, G. L., "The Effects of Pressure Gradients on Turbulent Flow Near a Smooth Wall," *Journal of Fluid Mechanics*, Vol. 24, Pt. 2, Feb. 1966, pp. 255–274.
- ² Smith, A. M. O. and Cebeci, T., "Numerical Solution of the Turbulent Boundary Layer Equations," Rept. DAC33735, 1967, Douglas Aircraft Div.
- ³ Patankar, S. V. and Spalding, D. B., "A Finite Difference Procedure for Solving the Equations of the Two-dimensional Boundary Layer," *International Journal of Heat and Mass Transfer*, Vol. 10, Oct. 1967, pp. 1389–1412.
- ⁴ Bradshaw, P., Ferriss, D. H., and Atwell, N. P., "Calculation of Boundary Layer Development Using the Turbulent Energy Equation," *Journal of Fluid Mechanics*, Vol. 28, Pt. 3, May 1967, pp. 593–616.
- ⁵ Lewkowicz, A. K. and Horlock, J. H., "An Implicit Approach to the Calculation of Two-dimensional Turbulent Boundary Layers," Rept. ULME/B19, 1966, Mechanical Engineering Dept., Liverpool Univ.

⁶ Hirst, E. A. and Reynolds, W. C., "An Integral Prediction Method for Turbulent Boundary Layers Using the Turbulent Kinetic Energy Equation," Rept. MD-21, 1968, Mechanical Engineering Dept., Stanford Univ.

⁷ Rotta, J. C., "Turbulent Boundary Layers in Incompressible Flow," *Progress in Aeronautical Sciences*, Vol. 2, Pergamon Press, 1962, pp. 1-220.

⁸ Head, M. R., "Entrainment in the Turbulent Boundary Layer," R. & M. 3152, 1958, Aeronautical Research Council.

⁹ Coles, D., "The Law of the Wake in the Turbulent Boundary Layer," *Journal of Fluid Mechanics*, Vol. 1, Pt. 2, July 1956, pp. 191-226.

¹⁰ Hinze, J. O., *Turbulence*, McGraw-Hill, New York, 1959.

¹¹ Kawasaki, T., "On an Approximate Solution of Two Dimensional Turbulent Boundary Layers," *Transactions of the Japan Society for Aeronautical and Space Sciences*, Vol. 4, No. 5, 1961, pp. 1-11.

¹² Clauser, F. H., "The Turbulent Boundary Layer," *Advances in Applied Mechanics*, Vol. 4, Academic Press, New York, 1956, pp. 1-51.

¹³ Goldberg, P., "Upstream History and Apparent Stress in Turbulent Boundary Layers," Rept. 85, 1966, Gas Turbine Lab., Massachusetts Institute of Technology.

¹⁴ McDonald, H., "The Departure from Equilibrium of Turbulent Boundary Layers," *Aeronautical Quarterly*, Vol. 19, Feb. 1968, pp. 1-19.

¹⁵ Nash, J. F. and Macdonald, A. G. J., "A Calculation Method for the Incompressible Turbulent Boundary Layer, Including the Effect of Upstream History on the Turbulent Shear Stress," Aero Rept. 1234, Dec. 1966, National Physical Lab.

¹⁶ Coles, D. and Hirst, E. A., 1968 *AFOSR-IFP Stanford Conference on Computation of Turbulent Boundary Layers, Proceedings*, Vol. 2, Stanford Univ.

¹⁷ Bradshaw, P. and Ferriss, D. H., "The Response of a Retarded Equilibrium Turbulent Boundary Layer to the Sudden Removal of Pressure Gradient," Aero Rept. 1145, 1965, National Physical Lab.

¹⁸ Townsend, A. A., "The Properties of Equilibrium Boundary Layers," *Journal of Fluid Mechanics*, Vol. 1, Pt. 6, Dec. 1956, pp. 561-573.

¹⁹ Cooke, J. C. and Hall, M. G., "Boundary Layers in Three Dimensions," *Progress in Aeronautical Sciences*, Vol. 2, Pergamon Press, 1962, pp. 221-282.

²⁰ Lewkowicz, A. K., "Two and Three Dimensional Incompressible Turbulent Boundary Layers," Ph.D. dissertation, 1965, Liverpool Univ.

²¹ Wakhaloo, C., "The End Wall Boundary Layer in a Compressor Cascade Passage," Ph.D. dissertation, 1968, Liverpool Univ.

²² Hoadley, D., "Three Dimensional Turbulent Boundary Layers in an Annular Diffuser," Ph.D. dissertation, 1969, Cambridge Univ.

²³ Cumpsty, N. A. and Head, M. R., "The Calculation of Three Dimensional Turbulent Layers, Part 1: Flow Over the Rear of a Swept Wing," *Aeronautical Quarterly*, Vol. 18, Feb. 1967, pp. 55-84.

²⁴ Bull, M. K., "Velocity Profiles of Turbulent Boundary Layers," *The Aeronautical Journal of the Royal Aeronautical Society*, Vol. 73, Feb. 1969, pp. 143-147.